

Hydration and Aggregation in Mono- and Disaccharide Aqueous Solutions by Gigahertz-to-Terahertz Light Scattering and Molecular Dynamics Simulations

L. Lupi,^{*,†} L. Comez,^{†,‡} M. Paolantoni,[§] S. Perticaroli,[§] P. Sassi,[§] A. Morresi,[§] B. M. Ladanyi,^{||} and D. Fioretto^{†,⊥}

[†]Dipartimento di Fisica, Università di Perugia, Via Pascoli, I-06123 Perugia, Italy

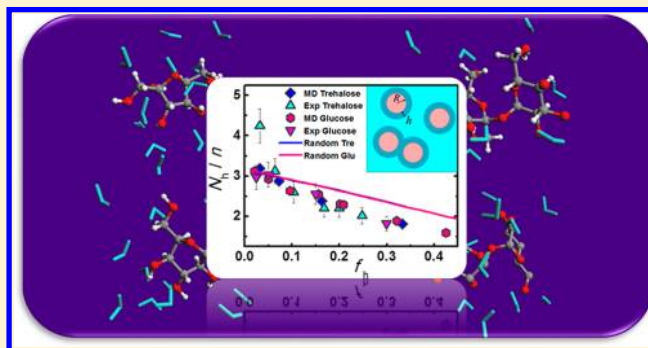
[‡]IOM-CNR c/o Dipartimento di Fisica, Università di Perugia, Via Pascoli, I-06123, Perugia, Italy

[§]Dipartimento di Chimica, Università di Perugia, Via Elce di Sotto, 8, I-06123 Perugia, Italy

^{||}Department of Chemistry, Colorado State University, Fort Collins, Colorado 80523-1872, United States

[⊥]Centro di Eccellenza sui Materiali Innovativi Nanostrutturati (CEMIN), Università of Perugia, via Elce di Sotto 8, 06123 Perugia, Italy

ABSTRACT: The relaxation properties of hydration water around fructose, glucose, sucrose, and trehalose molecules have been studied by means of extended frequency range depolarized light scattering and molecular dynamics simulations. Evidence is given of hydration dynamics retarded by a factor $\xi = 5\text{--}6$ for all the analyzed solutes. A dynamical hydration shell is defined based on the solute-induced slowing down of water mobility at picosecond time scales. The number of dynamically perturbed water molecules N_h and its concentration dependence have been determined in glucose and trehalose aqueous solutions up to high solute weight fractions (ca. 45%). For highly dilute solutions, about 3.3 water molecules per sugar hydroxyl group are found to be part of the hydration shell of mono- and disaccharide. For increasing concentrations, a noticeable solute-dependent reduction of hydration number occurs, which has been attributed, in addition to simple statistical shells overlapping, to aggregation of solute molecules. A scaling law based on the number of hydroxyl groups collapses the N_h concentration dependence of glucose and trehalose into a single master plot, suggesting hydration and aggregation properties independent of the size of the sugar. As a whole, the present results point to the concentration of hydroxyl groups as the parameter guiding both sugar–water and sugar–sugar interactions, without appreciable difference between mono- and disaccharides.



INTRODUCTION

Carbohydrates, together with water, play a fundamental role in many biological processes. Structural and dynamical properties of water–sugar solutions are believed to be responsible for peculiar bioprotective mechanism.^{1–3} For trehalose, in particular, it has been suggested that its strong bioprotectivity may be connected with the effect exerted by the sugar on the surrounding water.^{4,5} From a more general point of view, the great hydrogen bonding capability together with the high solubility in water makes carbohydrates particularly suitable for the study of the effects induced by a hydrophilic interface on the properties of water and on their modulation due to crowding effects. These latter are expected to be particularly relevant in intracellular processes.^{6,7} Thus, the study of these relatively simple systems over a range of concentrations might be helpful for deeper understanding of basic molecular properties of the so-called “biological water” (i.e., water surrounding complex biological macromolecules) important in various biochemical and biophysical processes.⁸

Raman and inelastic neutron scattering experiments^{9–13} showed pronounced destructuring effect on the ordered H-bond network of water. Among different disaccharides, trehalose has been found to be the most effective in modifying the typical water arrangements in connection with its greater bioprotective behavior.^{9,10} Other neutron diffraction studies supported by molecular dynamics (MD) simulation results suggested that the long-range structure of water is not significantly changed by the presence of glucose¹⁴ and that this sugar does not have a strong propensity to self-aggregate. Very recent neutron diffraction experiments indicated that the influence of trehalose on the water network is also surprisingly small¹⁵ and that, despite the number of available OH groups, only about four water molecules are H-bonded to each trehalose molecule.¹⁵ On the other hand, both experiments

Received: August 10, 2012

Revised: November 11, 2012

Published: December 3, 2012

and simulations observe a remarkable slowing down of the water mobility in sugar solutions^{16–18} often explained as being due to the formation of stable sugar–water hydrogen bonds.^{13,19} Moreover, the overall water dynamical retardation is found to strongly increase with the sugar concentration^{13,19} in analogy with what has been reported for a nonassociating amphiphile.⁷ Interestingly, in this work Stirnemann et al.⁷ pointed out that a greater slowing down on the overall water dynamics at increasing concentrations is strictly connected with a reduced self-association capability of the solute.

The changes imposed on the microscopic properties of water by the presence of the solute are expected to result in an observable modification of a macroscopic physical property of the solution.²⁰ On this basis an average solute hydration number N_h can be defined. It is well-known that reported N_h values may depend on the experimental method and/or on the assumptions adopted.²⁰ For example, density measurements, modeling the deviations from the “ideal” properties of the mixture have estimated N_h to be around 7 for dilute disaccharide solutions.²¹ Larger numbers have been deduced from viscosity and ultrasonic measurements,^{22–24} i.e., N_h ranging from 11 to 16 at room temperature. On the other hand, the number of water molecules H-bonded to sugars can also be obtained from MD simulations. Using the most common definition of the H-bond, in which two species are bonded if the oxygen–oxygen distance is less than 3.4 Å and the O–H...O angle is larger than 120°, numbers ranging from 15 to 18 at infinite dilution are obtained for trehalose,^{16,26–30} suggesting that experimental hydration numbers mainly refer to water molecules directly involved in H-bonds with the solute. The number of water–sugar H-bonds is found to decrease with increasing solute concentration when sugar–sugar contacts become important. Recently, a somewhat greater range of the dynamical perturbation, up to 5.5 Å, has been pointed out.¹⁶ An even longer range is deduced from terahertz (THz) experiments, where the concept of “dynamical hydration shell” has been introduced referring to water molecules perturbed at the picosecond and subpicosecond time scales. A slowing down extending up to 6–7 Å (two solvation layers) for the disaccharides lactose and trehalose is suggested, in contrast with a shorter-range perturbation of 3–4 Å (one solvation layer) deduced for the monosaccharide glucose,^{31,32} leading to the idea that the extent of solute influence grows with the molecular size. In these studies the relevance of sugar–water H-bonds in determining the long-range solvation dynamics was also pointed out. Very recently, Halle and co-workers³³ performed a detailed NMR investigation of trehalose aqueous solutions over a wide range of temperatures and concentrations. They report a modest slowing down effect of a factor of 1.6, induced by the sugar on the orientational dynamics of water molecules in the first solute hydration layer.

Within this framework, the combined use of MD simulations and extended frequency range depolarized light scattering (EDLS) experiments might be helpful in addressing the following issues: How large is the dynamical perturbation induced by the sugars, and what is its spatial extent? Where are the perturbed molecules located? Is the hydration dynamics sugar dependent? Is it concentration dependent? What is the role played by eventual aggregation phenomena?

In recent publications we demonstrated the suitability of EDLS experiments, performed in the frequency range going from ~ 0.3 to 3×10^4 GHz combining dispersive and interferometric setups, for the study of hydration dynamics in

biorelevant systems.^{12,34–40} In particular, in these works it has been shown that the analysis of EDLS spectra provides the retardation ratio ξ between the relaxation times of hydration (several picoseconds) and bulk water, typically ranging from about 4 to 10 around room temperature, and the corresponding hydration number, namely, the number of water molecules belonging to the solute dynamical hydration shell. In the present work we extend our investigation to several water–sugar systems, allowing an overall comparison between mono- and disaccharides (fructose, glucose, sucrose, and trehalose). Additionally, the concentration dependence of N_h of glucose and trehalose is analyzed in greater detail.

METHODS

Experimental Section. Sucrose was purchased from Panreac with purity higher than 99.1%. Trehalose, glucose, and fructose were purchased from Fluka Sigma-Aldrich with purities higher than 99.5%. The solutions were prepared by weight, adding sugar to water doubly distilled and deionized in our laboratory, then stirring and heating until the solute was completely dissolved. All the solutions were freshly prepared and conditioned for more than 1 h in a 10 mm path quartz cuvette before EDLS measurements were made. Vertically polarized single mode Ar⁺ ($\lambda_0 = 514.5$ nm) and solid state ($\lambda_0 = 532$ nm) lasers were used as light sources with typical power lower than 500 mW, and the horizontally polarized scattered light (I_{VH}) was analyzed by means of two different spectrometers.

The low-frequency region from 0.3 to 200 GHz was recorded in back scattering geometry, by means of a Sandercock-type (3 + 3)-pass tandem Fabry–Perot interferometer, characterized by a finesse of about 100 and a contrast $> 5 \times 10$.¹⁰ Three different mirror separations, $d = 14$ mm, $d = 4$ mm, and $d = 1$ mm, corresponding to distinct free spectral ranges, were used. Data acquisition was performed by means of a system developed and tested in our laboratory, composed by an electronic board connected to the interferometer control unit, and by a dedicated software running inside the board and on a laboratory PC. The software running on the acquisition PC is a dialogue-based application, named GHOST, working as an advanced multichannel analyzer.⁴¹

Higher frequency measurements were recorded in the 3–36 000 GHz ($1\text{--}1200\text{ cm}^{-1}$) frequency range using an ISA Jobin-Yvon model U1000 double monochromator having 1 m focal length with holographic gratings. The detection system utilized was a thermoelectrically cooled Hamamatsu model 943XX photomultiplier, computer-controlled by the ISA Jobin-Yvon SpectraMax package. The scattered light was collected adopting a 90° scattering geometry in two different frequency regions: from -10 to 40 cm^{-1} with a resolution of 0.5 cm^{-1} and from 3 to 1200 cm^{-1} with a resolution of 1 cm^{-1} .

After subtraction of the dark count contribution, low- and high-frequency spectra were spliced taking advantage of an overlap of about half a decade in frequency. Further, the susceptibility spectra $\chi''(\nu)$ were calculated as the ratio between the $I_{VH}(\nu)$ intensity and $[n(\nu) + 1]$, where $n(\nu)$ is the Bose–Einstein occupation number, namely $n(\nu) = [\exp(h\nu/kT) - 1]^{-1}$.

Computational Section. We have carried out MD simulations of aqueous solutions of glucose and trehalose at room temperature and at several concentrations. The interaction model and MD simulation method that we used in the case of trehalose have been described elsewhere.⁴² A

similar procedure and the same type of interaction model were used for glucose solutions. Specifically, MD simulation was carried out using the DL_POLY2.0 package.^{43,44} The MD trajectories were generated using the SPC/E potential model for water⁴⁵ and the optimized potential for liquid simulation (OPLS) all-atom force field for carbohydrates, developed by Jorgensen and co-workers,⁴⁶ for both trehalose and glucose. The SPC/E model treats the molecules as nonpolarizable, rigid bodies, interacting via a pairwise sum of site–site interactions involving electrostatic terms between fixed partial charges and Lennard-Jones (LJ) interactions, with a single LJ site on the oxygen atom. Within the all-atom OPLS model,⁴⁶ trehalose and glucose are represented by 45 and 23 interaction sites, respectively, and modeled as a fully flexible molecules. Bonded interactions include stretching, bending and torsional potentials. The nonbonded interactions include Coulombic and LJ potentials between atoms separated by at least three bonds within the same carbohydrate molecule and between atoms on different molecules. For atoms separated by three bonds within a glucose or a trehalose molecule, the nonbonded interaction is decreased by a factor of 2. The OPLS model was chosen for this study because it is a relatively simple, pairwise-additive, potential that has been shown to be accurate for the properties of mono- and disaccharide aqueous solutions relevant to the present application.^{16,28} Interatomic distances within water molecules were kept fixed by using the SHAKE iterative procedure.⁴⁷ This constraint method was used to integrate the equations of motion of the rigid molecules, in combination with the velocity Verlet algorithm, with a time step of 1 fs. We have considered, in addition to the pure water, aqueous mixtures having trehalose mole fractions of $X_{\text{TRE}} = 0.004, 0.009, 0.02,$ and 0.04 and glucose mole fractions of $X_{\text{GLU}} = 0.004, 0.01, 0.019, 0.03, 0.039, 0.04, 0.06,$ and 0.078 . The simulations were performed in the microcanonical ensemble with a total number of $N = 200$ – 250 molecules placed in a cubic box with periodic boundary conditions. Short-ranged intermolecular interactions were cut off at half the box length, while standard Ewald sums with conducting boundaries were used to handle long-range Coulombic forces.⁴⁸ Preliminary trajectories of 200 ps in the NPT ensemble were first run in order to equilibrate the system at 27°C K and 1 atm. Production runs of 2 ns each were then generated in the microcanonical ensemble.

RESULTS AND DISCUSSION

Figure 1 shows EDLS spectra of pure water and solutions of monosaccharides (fructose and glucose) and disaccharides (trehalose and sucrose) at $T = 25^\circ\text{C}$. Because of the presence of the sugar, new spectral features arise in the high (>10 THz) and low (<1 THz) frequency regions of the spectrum, while the 1–10 THz region is only marginally affected by the solute. The high-frequency features can be attributed to intramolecular resonant modes of sugar molecules and to librational modes of water.³⁶ On the opposite side, for frequencies lower than about 10 GHz, the spectrum is dominated by a relaxation attributed to the rotational diffusion of sugar molecules. Intensity variations of this peak observed for the different samples suggest a larger optical anisotropy of glucose and trehalose with respect to fructose and sucrose, respectively. Also, notice the factor of about 2 between the characteristic frequency of the peak of mono- and disaccharides due to the different molecular hydrodynamic volumes.^{35,38} The region between 1 and 10 THz is assigned to the intermolecular bending and stretching resonant modes of the water molecules.³⁶ The depicted spectra

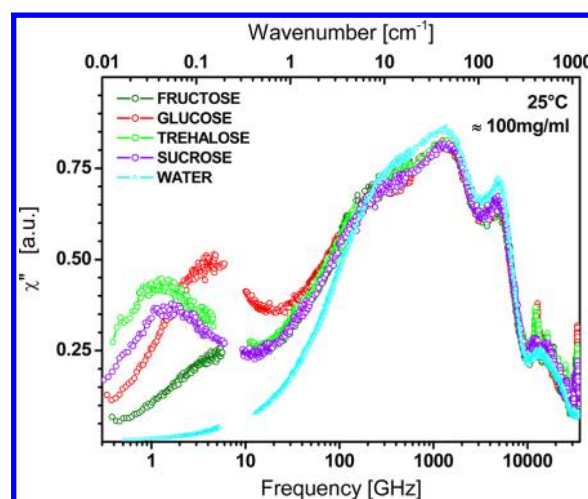


Figure 1. Imaginary part of the susceptibility of pure water and of aqueous solutions of monosaccharides (fructose and glucose) and disaccharides (trehalose and sucrose) at the same concentration 100 mg/mL and at 25°C . The lack of data around 10 GHz is due to the removal of few spurious points originating from the leakage of the Brillouin peaks.

were arbitrarily rescaled on the librational band of water, which is weakly affected by the presence of different solutes and also by temperature changes.¹²

Hydration Properties. Relevant information on structure and dynamics of water molecules in solution can be inferred from the spectral region extending from about 10 to 10^3 GHz, which includes the characteristic relaxation of water.³⁷ Because of the slow exchange condition,⁴⁹ two distinct relaxation processes can be identified in this region:^{34,37,38} a fast process related to bulk water molecules scarcely affected by the solute and a slower one related to hydration molecules. The possibility of disentangling the dynamics of hydration water from that of the solute and bulk water contributions is an important achievement of EDLS, which makes it a technique of great potential in the study of biological water. To better emphasize the modifications induced by the sugars on the spectral distributions, in Figure 2 are shown the solvent-free (SF) spectra, obtained by subtracting the susceptibility of water from those of the solutions.

In this representation, the prominent spectral features are the low-frequency peaks arising from the rotational diffusion of sugar molecules and the additional contribution that, for all the samples, is centered at $\nu \approx 60$ GHz, corresponding to a relaxation time of about 2.5 ps. As recently confirmed by molecular dynamics simulations,⁴² the latter relaxation process can be attributed to hydration water. We note that the water residence time within the fructose hydration shell, estimated by MD simulations from the water–fructose hydrogen bond survival time-correlation function, is found to be larger than 20 ps,¹⁷ while a characteristic value of the order of 10 ps is inferred on the basis of the rotational relaxation time of water in the trehalose shell measured by NMR.³³ The fact that the relaxation detected here is considerably faster (2.5 ps) than the estimated residence time supports its assignment to the dynamics of water molecules temporally located within the sugar hydration layer and the validity of the slow exchange condition for this process. Considering that the main relaxation process in pure water has a characteristic time of about 0.5 ps, a 5-fold retardation effect on hydrating molecules can be

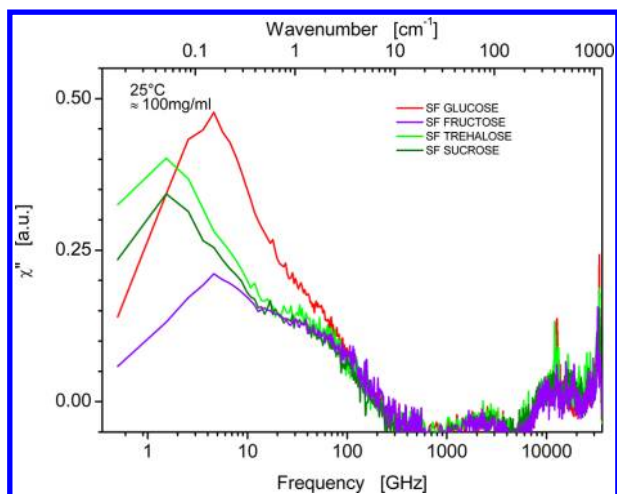


Figure 2. Solvent-free spectra for the sugar/water susceptibilities of Figure 1. The contribution of bulk water has been subtracted to emphasize the contributions of sugars and of hydration water.

estimated. The position and the width of the peak corresponding to this relaxation process are surprisingly independent from the solute, i.e., from the position and intensity of the sugar rotational contribution, providing additional evidence of the fact that the molecular origin of this process is to be found in the dynamics of solute-perturbed water molecules, rather than in the dynamics of the sugar molecules themselves. Moreover, it can be argued from Figure 2 that the amplitude of the water relaxation spectral component is also nearly independent of the type of solute, as will be discussed in detail below.

Following the indications coming from the spectra reported above, a phenomenological model has been applied to extract relaxation times and amplitudes of the different spectral features. With this aim, the susceptibility spectrum has been modeled as the sum of five distinct contributions, as reported in Figure 3. Three Cole–Davidson functions are used to fit the relaxation components: the one located at few units of GHz accounts for the rotational dynamics of the sugar, while the

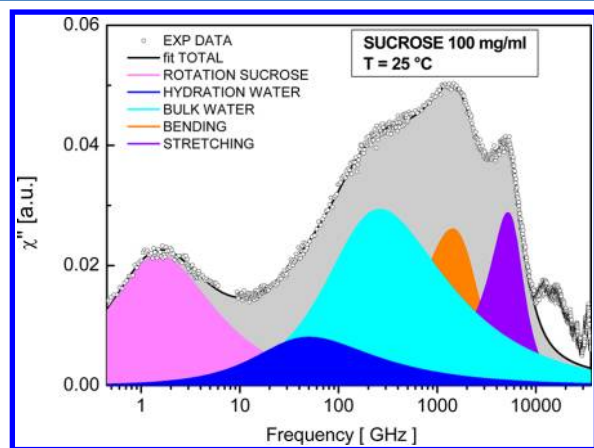


Figure 3. Susceptibility of the 100 mg/mL sucrose/water solution at 25 °C. Experimental data (black circles) are reported together with the total fitting curve (black line) and individual components: rotational diffusion of sucrose (pink); relaxation of hydration (blue) and bulk (cyan) water; and bending and stretching intermolecular resonant modes of water (orange and violet).

components centered at about 60 and 300 GHz are associated with the relaxation process of hydration and bulk water molecules, respectively. Finally, two damped harmonic oscillator (DHO) functions are used to represent the two resonant modes of the H-bonded water network, located around 1800 and 5100 GHz (i.e., 60 and 170 cm^{-1}). As a whole, the fitting function for our spectra is

$$\chi''(\omega) = \text{Im} \left\{ -\frac{\Delta_T}{[1 + i\omega\tau_T]^{\beta_T}} - \frac{\Delta_{\text{slow}}}{[1 + i\omega\tau_{\text{slow}}]^{\beta_{\text{slow}}}} - \frac{\Delta_{\text{fast}}}{[1 + i\omega\tau_{\text{fast}}]^{\beta_{\text{fast}}}} + \frac{\Delta_b \omega_b^2}{\omega^2 - \omega_b^2 - i\omega\Gamma_b} + \frac{\Delta_s \omega_s^2}{\omega^2 - \omega_s^2 - i\omega\Gamma_s} \right\} \quad (1)$$

where in the first three additive terms Δ_j is the amplitude, τ_j the relaxation time, and β_j the stretching parameter. The subscript $j = T$ refers to the sugar relaxation term, while the subscripts $j = \text{slow}$ and $j = \text{fast}$ refer respectively to the relaxation terms for the hydration and bulk-like water. The possible nonexponential decay of these three relaxation functions is taken into account through the value of the parameter $\beta_j < 1$. The remaining two additive terms correspond to intermolecular bending (b) and stretching (s) modes of water, which are represented as Lorentzians with characteristic frequencies ω_b and ω_s , amplitudes Δ_b and Δ_s , and widths Γ_b and Γ_s .

Figure 3 depicts a representative spectrum fitted by eq 1 and illustrates its five contributions. In the present work we focus our attention on the two central peaks attributed to hydration and bulk water. These relaxation processes should essentially relate to the local translational motion of water molecules that modulate the anisotropic polarizability of the system via intermolecular interaction-induced mechanisms. As recently shown for water–trehalose mixtures,⁴² rotational contributions of water to the spectrum are of minor importance with respect to translational ones owing to the almost isotropic polarizability of water molecules. The structural rearrangements of water are closely related to the fast hydrogen bond reorganization of the system, and the corresponding relaxation time is often regarded as a measure of the average hydrogen bond lifetime.^{12,36,50,51}

In the fitting procedure, the values of the stretching parameters β_{slow} and β_{fast} have been fixed to value for pure water ($\beta = 0.6$),^{12,37} and the relaxation times and amplitudes are left free, after a first fitting run in which the relaxation time τ_{fast} is fixed to its value in bulk water, the value finally obtained for τ_{fast} is compatible, within experimental error, with that of bulk water, with a weak tendency to increase for increasing solute concentration. This two-step fitting procedure is especially useful in the case of aqueous glucose solutions, where the intense peak due to the sugar rotational relaxation tends to mask the water contribution (see Figure 2).

Figure 4 displays the retardation ratio ξ obtained for the different solutions of Figure 1. It can be seen that, consistent with the previous evaluation from Figure 2, these values are within 5–6 for all four sugars. It is important to notice that the estimated retardation factors do not depend on the fitting strategy and, in particular, on the value of the stretching parameters, as long as the constraint $\beta_{\text{slow}} = \beta_{\text{fast}}$ is retained. The value of $\xi \cong 5$ –6 observed here for mono- and disaccharides is intermediate between higher values, $\xi \cong 7$ –8, obtained for

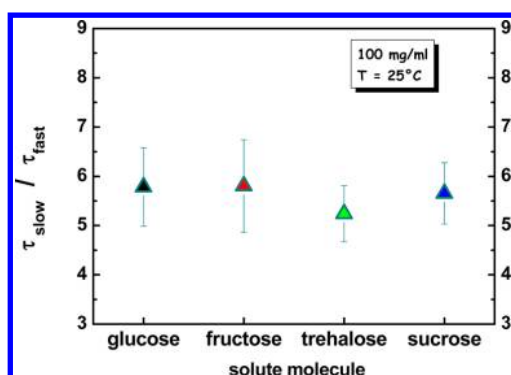


Figure 4. Retardation factors $\xi = \tau_{\text{slow}}/\tau_{\text{fast}}$ for aqueous solutions of monosaccharides (fructose and glucose) and disaccharides (trehalose and sucrose). Relaxation times of the hydrating τ_{slow} and bulk τ_{fast} water relaxation processes are obtained by the adopted fitting procedure.

peptides and proteins^{39,40} and slightly smaller values obtained for hydrophobic molecules^{52–54} using different approaches.

Dynamical Hydration Shell. To gain more insight into hydration properties of mono- and disaccharides, a more detailed analysis of the spectral data of glucose and trehalose aqueous solutions at different concentrations is reported in the following. In particular, EDLS spectra of glucose solutions at $T = 35^\circ\text{C}$, analyzed in refs 12 and 38 in terms of a single water relaxation term, are now reanalyzed using the two-step fitting procedure described above. The results are compared with those reported in ref 42 for trehalose solutions at the same temperature and in a similar concentration range. Concerning the water dynamics, the estimated retardation factor is almost concentration-independent for both samples.^{42,55} On the contrary, the number of water molecules dynamically perturbed by each solute (hydration number N_h , reported here in Figure 5) is found to strongly depend on both sample and concentration. The value of N_h is obtained from EDLS spectra as the fraction of water molecules contributing to the slow relaxation term divided by the sugar/water molar ratio f_s , i.e., $N_h = \Delta_{\text{slow}}/[f_s(\Delta_{\text{slow}} + \Delta_{\text{fast}})]$. Figure 5 shows a systematic

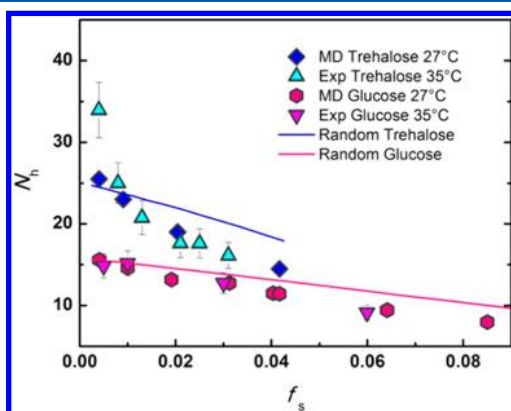


Figure 5. Hydration numbers N_h computed from MD trajectories, obtained by considering water molecules whose oxygen is within a distance $r = 3.6 \pm 0.1$ Å from the oxygen of each solute hydroxyl group, reported together with experimental N_h values for both glucose and trehalose solutions as functions of concentration. Continuous lines refer to N_h values calculated using a simple numerical method based on the generation of random distributions of solute-like molecules in water; see text for details.

reduction of N_h for increasing solute concentration, with a more pronounced variation for trehalose. We note that in previous work on trehalose³⁷ this behavior was not emphasized, and only the N_h value of ca. 17, obtained by averaging over concentrations, was discussed. Previous computational studies reported a similar behavior to that shown in Figure 5 for the concentration dependence of sugar hydration number.²⁹ In those studies the numbers of water molecules directly hydrogen bonded with the solute were computed, leading to absolute values smaller than those of Figure 5. This suggests that the dynamical perturbation probed by EDLS extends over a larger number of water molecules, pointing out the need for a different definition of the hydration shell. To this end, MD simulation for both glucose and trehalose solutions (at a specific temperature and several concentrations; see Methods), are performed, and the geometrical condition for the hydration number matching experimental results is defined. Using this procedure, values in agreement with experimental ones are derived, through the whole concentration range, considering those water molecules whose oxygen (O_w) is within a distance $r = 3.6 \pm 0.1$ Å from the oxygen (O_s) of a solute hydroxyl group (OH_s). Remarkably, the same distance criterion is found for both glucose and trehalose. The resulting computed values together with the experimental ones are reported in Figure 5 as a function of f_s . It should be noted that the O_w – O_s distance used in our calculations is close to the value of the first minimum in the O_w – O_s radial distribution function of water–sugar solutions.¹⁶

Similar concentration behavior of N_h is recovered if one selects water molecules with O_w distance smaller than 3.1 Å from any solute atom. It is not surprising that the two definitions of hydration water give the same results in the case of glucose and trehalose, in which hydroxyl groups are almost uniformly distributed all around the surface of the molecules. A recent MD investigation showed that the water molecules selected with this geometrical criterion do exhibit retarded dynamics at picosecond time scales.⁵⁶

As a whole, our results demonstrate that sugar molecules influence the picosecond water mobility at relatively short distances (3–4 Å) encompassing a number of water molecules exceeding those instantaneously hydrogen bonded with the solute. Remarkably, a similar short-range dynamical restriction, essentially confined to the first hydration layer, is found independently on the sugar size.

These findings seem to contradict THz experiments from which, in the case of trehalose, a longer range perturbation extending over two water layers was estimated.³² However, differences between our results and theirs indicate mainly that the two experiments probe different system properties. As already pointed out,³⁷ even though THz experiments, which probe dipolar relaxation at subpicosecond time scales (or resonant intermolecular vibrations at around 2.5 THz), might have somewhat larger sensitivity to minor dynamical perturbations, our results confirm that, concerning the picosecond relaxation properties of the polarizability anisotropy, glucose and trehalose affect similarly the dynamics within the first hydration layer.

Moreover, from the hydration numbers calculated for a single solute molecule in water (infinite dilution) for trehalose ($N_h = 25$) and glucose ($N_h = 16$), a ratio very close to 8/5, ratio between the numbers of hydroxyl groups of the two sugar molecules, is obtained and an average value of about 3.3 water molecules per OH_s is found to be dynamically retarded for both

dilute systems. In line with these observation, Figure 6 shows a plot of the normalized hydration numbers N_h/n as a function of

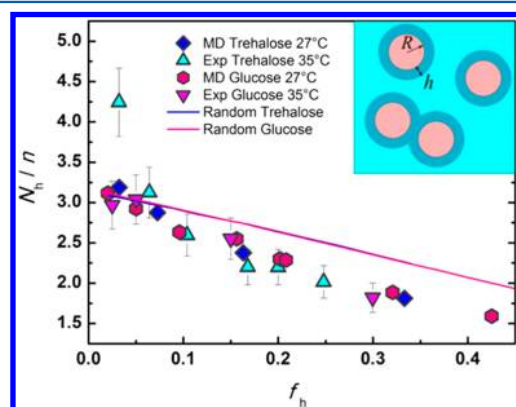


Figure 6. Normalized hydration numbers N_h/n as a function of the OH_s/water mole ratio $f_h = n f_s$, where n is the number of OH_s for each sugar molecule.

the OH_s/water mole ratio $f_h = n f_s$, where n is the number of OH_s groups for each sugar molecule and $f_s = n_s/n_w$ is the sugar/water mole ratio. It can be seen that, in this representation, all the data collapse into a single master plot, suggesting that the number of hydroxyl groups is, indeed, the relevant parameter for the hydration process in the whole concentration range.

Referring to the solvent-free spectra of Figure 2, the observation that for different sugars the slow water relaxation shows similar amplitudes can be now rationalized in terms of the reported scaling behavior. In fact, a similar concentration of solute in water (100 mg/mL) corresponds to similar OH_s/water mole ratios for the different sugars.

Aggregation Properties. The origin of the decrease of N_h as a function of sugar concentration will be now discussed in greater detail. The observed dependence can be explained in terms of superposition of hydration shells of different solute molecules (see inset of Figure 6), which is expected to increase with increasing concentration, leading to a progressive reduction in the average hydration number. This behavior can result either from a simple statistical effect or from incipient aggregation phenomena. Even in the absence of any clustering tendency, i.e., for a random distribution of solute molecules, a nonzero probability of shell intersection is expected. To quantify the contribution of this basic effect on the concentration dependence of N_h , a simple numerical method based on the generation of random distributions of solute-like molecules in water is adopted. In particular, for any given mole fraction, several random distributions of solute molecules are generated in a simulation box containing water molecules at the appropriate density. The glucose-like molecule is a sphere of radius R estimated from the hydrodynamic volume V previously obtained by EDLS experiments,^{35,38} namely $R = (3V/4\pi)^{1/3} = 3.41$ Å. The trehalose-like molecule is represented as the composite of two glucose-like spherical units at a fixed 4 Å center–center distance. The chosen dimensions give a reasonable estimate for the axial ratio of the trehalose molecule as well as the solvent-exposed surface for trehalose 1.6-fold greater than the one for glucose. Moreover, an effective hydration shell of constant thickness h ($h = 1.94$ Å for glucose and $h = 2.06$ Å for trehalose) is determined in the case of a single sugar molecule in the aqueous medium (highest dilution), such that the number of water molecules located

within this shell equals the hydration numbers derived by MD simulations. Using this schematic model, the values of N_h determined by averaging over several random configurations are then evaluated as a function of concentration and reported in Figure 5 as full lines. The renormalized values N_h/n are also reported as full lines in Figure 6. The obtained trend is merely the result of a geometric effect related to the random superposition of different shells (overlap volumes) and does not account for any particular interaction mechanism between sugar molecules. It is noteworthy that the obtained hydration numbers decrease with increasing concentration at slower rates in comparison with both experimental and MD counterparts, suggesting that the random intersection of hydration shells is not sufficient to fully account for the observed effect. Thus, specific intermolecular interactions, which favor solute aggregation at increasing concentrations, also contribute toward reducing the effective values of the hydration numbers. In addition, the scaling behavior reported in Figure 6 indicates that the solute self-association statistics are analogous for glucose and trehalose systems, in line with their similar hydrogen-bonding character.

Evidence of the formation of trehalose–trehalose hydrogen bonds in aqueous solutions has been reported in recent computational studies,^{13,30} while solute aggregation effects have also been found by means of photon correlation spectroscopy measurements in aqueous solutions of glucose at lower temperatures.⁵⁷ The existence of direct trehalose–trehalose interactions at sugar concentrations well below those examined here has recently been detected by NMR spectroscopy.³³

CONCLUSIONS

EDLS experiments and MD simulations have been used to gain information both on the number of water molecules dynamically perturbed by monosaccharides (glucose and fructose) and disaccharides (sucrose and trehalose) and on the identity of the dynamical perturbation. It is worth noting that the possibility of measuring both these parameters is a peculiar characteristic of EDLS, since it gives access to a spectral range large enough to comprise the rotational diffusion of the solute as well as the relaxation and the vibrational features of the hydrogen bonds. Moreover, unlike other spectroscopic techniques, EDLS reveals the relaxation of water at frequencies much higher than the exchange rate between hydration and bulk water (slow exchange condition) so that both relaxation times and amplitudes can be directly obtained from the spectra, without the need for ad-hoc assumptions.

The retardation factor ξ induced by carbohydrates on the picosecond rearrangement of surrounding water is found to be 5–6 and to depend neither on the particular system nor on the concentration. This is particularly surprising at the higher concentrations investigated reaching ca. 50 wt %. The dynamical hydration shell, defined as the region around the solute that includes water molecules retarded at picoseconds time scales, has been characterized. In the most dilute condition, about 16 (25) water molecules result dynamically perturbed per glucose (trehalose) unit, such that each hydroxyl group constraints the dynamics of about 3.3 solvent molecules ($N_h/n \cong 3.3$). It is worth noting that retarded water molecules exceeds the number of those instantaneously H-bonded to the sugar, which corresponds to about 1.8 water molecules per sugar OH, for both glucose and trehalose.¹⁶ Thus, from the present investigation emerges a dynamical hydration shell,

comprising solvent molecules within a radius of about 3.6 Å from the oxygen of each sugar hydroxyl group (or equally of about 3.1 Å from each solute atom), suggesting a relatively short-range effect for both mono- and disaccharides. For the sake of comparison, we remark that in previous EDLS experiments performed for peptide and protein aqueous solutions larger retardation factors and more extended dynamical hydration shells were found,^{39,40} reinforcing the notion that glucose and trehalose fit quite well into the hydrogen bond network of water.

The short-range effect exerted by trehalose on the water dynamics is in general agreement with NMR results of Halle and co-workers.³³ However, these authors found a smaller dynamical retardation factor of 1.67. This difference can be partially explained considering that NMR experiments probe single molecule rotational motion of water molecules while the dynamics detected by EDLS is related to a collective structural rearrangement of water, mainly connected with molecular translations.⁴² Thus, in principle, a solute might influence to a different extent these physically distinct processes, even if order of magnitude discrepancies are not expected in water owing to the common role played by hydrogen bond reorganization dynamics. Some of us recently showed that the water contribution to the total relaxation of the anisotropic polarizability decay is dominated by interaction-induced contribution (translations) in the whole concentration range and that this term is more strongly affected by the retardation when compared to the molecular component sensitive to water rotations.⁴² It is worth mentioning here that in a recent MD study⁵⁸ the time correlation function of fluctuations in N , the hydration number within 3.5 Å of each trehalose oxygen, has been calculated, leading to retardation factors for density fluctuations of 9.5 for water molecules next to the glycosidic oxygen, 3 for molecules near ether oxygens, and 2 for the other ones. In the same work a maximum retardation factor of 4.4 is reported for the rotational anisotropy decay of hydrating water. We also mention that the NMR retardation factor of 1.67 is obtained for very dilute samples ($f_s < 0.004$),³³ in a concentration range where hydration shell superposition effects are likely to be negligible. A larger perturbation factor is predicted by the authors at $f_s > 0.004$ to explain the superlinear concentration dependence of the water relaxation rate.

We found a noticeable concentration dependence of the hydration numbers has been found in both glucose and trehalose solutions. A simple scaling law is proposed, based on the number n of OH_s groups, which allows one to collapse the concentration dependence of N_h of both mono- and disaccharide into a single master plot. An almost linear reduction of N_h/n is observed on increasing OH_s/water mole ratio; moreover, N_h/n halves its value going from 0 to 0.3, underscoring the key role played by OH groups, in analogy with the results obtained by THz experiments³² and viscosity measurements.³⁵ These findings demonstrate a nonspecific solvation effect in going from glucose to trehalose. Moreover, it is surprising that, when crowding condition are reached, a large population of bulk-like water molecules still exists, namely at the highest solute concentrations (ca. 50 wt %) about 40% of the water available is outside the dynamical hydration shell. This picture seems to be consistent with the formation of water pools at high solute concentration observed in a recent MD simulation.¹⁷

To provide a rationale for the detected concentration behavior of N_h , a simple numerical method is proposed

aimed at evaluating the finite overlap probability of randomly distributed hydration shells. This model predicts a slower decrease in N_h with increasing sugar concentration than is found from both MD simulation and experiments. This discrepancy may be attributed to the occurrence of solute aggregation effects. Interestingly, a similar aggregation picture is found in glucose and trehalose solutions as substantiated by the rescaled master plot.

Overall, our results suggest that the concentration of hydroxyl groups is the relevant parameter, guiding both water–sugar and sugar–sugar interactions, and no specific effect of trehalose has been detected that can provide an explanation for the better bioprotective features of this disaccharide. EDLS measurements and simulations performed near the freezing point of water–sugar–biomolecule ternary mixtures might help to clarify this point.

AUTHOR INFORMATION

Corresponding Author

*E-mail laura.lupi@fisica.unipg.it.

Notes

The authors declare no competing financial interest.

ACKNOWLEDGMENTS

We thank Francesco Sciortino and Dmitry Matyushov for helpful discussions. B.M.L. gratefully acknowledges the U.S. National Science Foundation, Grant CHE-0911668, for partial support of this research.

REFERENCES

- (1) Crowe, J. H.; Crowe, L. M.; Chapman, D. *Science* **1984**, *223*, 701–703.
- (2) Carpenter, J. F.; Crowe, J. H. *Biochemistry* **1989**, *28*, 3916–3922.
- (3) Crowe, J. H.; Crowe, L. M. *Nat. Biotechnol.* **2000**, *18*, 145–146.
- (4) Magazù, S.; Villari, V.; Migliardo, P.; Maisano, G.; Telling, M. T. *F. J. Phys. Chem. B* **2001**, *105*, 1851–1855.
- (5) Massari, A. M.; Finkelstein, I. J.; McClain, B. L.; Goj, A.; Wen, X.; Bren, K. L.; Loring, R. F.; Fayer, M. D. *J. Am. Chem. Soc.* **2005**, *127*, 14279–14289.
- (6) Ellis, R. J.; Minton, A. P. *Nature* **2003**, *425*, 27–28.
- (7) Stirnemann, G.; Sterpone, F.; Laage, D. *J. Phys. Chem. B* **2011**, *115*, 3254–3262.
- (8) Pal, S. K.; Peon, J.; Zewail, A. H. *Proc. Natl. Acad. Sci. U. S. A.* **2002**, *99*, 15297–15302.
- (9) Branca, C.; Magazù, S.; Maisano, G.; Migliardo, P. *J. Chem. Phys.* **1999**, *111*, 281–287.
- (10) Branca, C.; Magazù, S.; Maisano, G.; Bennington, S. M.; Fak, B. *J. Phys. Chem. B* **2003**, *107*, 1444–1451.
- (11) Perticaroli, S.; Sassi, P.; Morresi, A.; Paolantoni, M. *J. Raman Spectrosc.* **2008**, *39*, 227–232.
- (12) Paolantoni, M.; Comez, L.; Fioretto, D.; Gallina, M. E.; Morresi, A.; Sassi, P.; Scarponi, F. *J. Raman Spectrosc.* **2008**, *39*, 238–243.
- (13) Lerbret, A.; Affouard, F.; Bordat, P.; Hedoux, A.; Guinet, Y.; Descamps, M. *J. Non-Cryst. Solids* **2011**, *357*, 695–699.
- (14) Mason, P. E.; Neilson, G. W.; Enderby, J. E.; Sabounji, M. L.; Brady, J. W. *J. Phys. Chem. B* **2005**, *109*, 13104–13111.
- (15) Pagnotta, S. E.; McLain, S. E.; Soper, A. K.; Bruni, F.; Ricci, M. A. *J. Phys. Chem. B* **2010**, *114*, 4904–4908.
- (16) Lee, S. L.; Debenedetti, P. G.; Errington, J. R. *J. Chem. Phys.* **2005**, *122*, 204511.
- (17) Sonoda, M. T.; Skaf, M. S. *J. Phys. Chem. B* **2007**, *111*, 11948–11956.
- (18) Magno, A.; Gallo, P. *J. Phys. Chem. Lett.* **2011**, *2*, 977–982.
- (19) Pomata, M. H. H.; Sonoda, M. T.; Skaf, M. S.; Elola, M. D. *J. Phys. Chem. B* **2009**, *113*, 12999–13006.
- (20) Burakowski, A.; Glinski, J. *Chem. Rev.* **2012**, *112*, 2059–2081.

- (21) Gharsallaoui, A.; Roge, B.; Genotelle, J.; Mathlouthi, M. *Food Chem.* **2008**, *106*, 1443–1453.
- (22) Galema, S. A.; Hoiland, H. J. *Phys. Chem.* **1991**, *95*, 5321–5326.
- (23) Magazù, S.; Migliardo, P.; Musolino, A. M.; Sciortino, M. T. *J. Phys. Chem. B* **1997**, *101*, 2348–2351.
- (24) Branca, C.; Magazù, S.; Maisano, G.; Migliardo, F.; Migliardo, P.; Romeo, G. *J. Phys. Chem. B* **2001**, *105*, 10140–10145.
- (25) Brady, J. W.; Schmidt, R. K. *J. Phys. Chem.* **1993**, *97*, 958–966.
- (26) Liu, Q.; Schmidt, R. K.; Teo, B.; Karplus, P. A.; Brady, J. W. *J. Am. Chem. Soc.* **1997**, *119*, 7851–7862.
- (27) Bonanno, G.; Noto, R.; Fornili, S. L. *J. Chem. Soc., Faraday Trans.* **1998**, *94*, 2755–2762.
- (28) Conrad, P. B.; de Pablo, J. J. *J. Phys. Chem. A* **1999**, *103*, 4049–4055.
- (29) Lerbret, A.; Bordat, P.; Affouard, F.; Descamps, M.; Migliardo, F. *J. Phys. Chem. B* **2005**, *109*, 11046–11057.
- (30) Sapir, L.; Harries, D. J. *Phys. Chem. B* **2011**, *115*, 624–634.
- (31) Heugen, U.; Schwaab, G.; Brundermann, E.; Heyden, M.; Yu, X.; Leitner, D. M.; Havenith, M. *Proc. Natl. Acad. Sci. U. S. A.* **2006**, *103*, 12301–12306.
- (32) Heyden, M.; Brundermann, E.; Heugen, U.; Niehues, G.; Leitner, D. M.; Havenith, M. *J. Am. Chem. Soc.* **2008**, *130*, 5773–5779.
- (33) Winther, L. R.; Qvist, J.; Halle, B. J. *Phys. Chem. B* **2012**, *116*, 9196–9207.
- (34) Rossi, B.; Comez, L.; Fioretto, D.; Lupi, L.; Caponi, S.; Rossi, F. *J. Raman Spectrosc.* **2011**, *42*, 1479–1483.
- (35) Gallina, M. E.; Comez, L.; Morresi, A.; Paolantoni, M.; Perticaroli, S.; Sassi, P.; Fioretto, D. *J. Chem. Phys.* **2010**, *132*, 214508.
- (36) Paolantoni, M.; Sassi, P.; Morresi, A.; Santini, S. J. *Chem. Phys.* **2007**, *127*, 024504.
- (37) Paolantoni, M.; Comez, L.; Gallina, M. E.; Sassi, P.; Scarponi, F.; Fioretto, D.; Morresi, A. *J. Phys. Chem. B* **2009**, *113*, 7874–7878.
- (38) Fioretto, D.; Comez, L.; Gallina, M. E.; Morresi, A.; Palmieri, L.; Paolantoni, M.; Sassi, P.; Scarponi, F. *Chem. Phys. Lett.* **2007**, *441*, 232–236.
- (39) Perticaroli, S.; Comez, L.; Paolantoni, M.; Sassi, P.; Lupi, L.; Fioretto, D.; Paciaroni, A.; Morresi, A. *J. Phys. Chem. B* **2010**, *114*, 8262–8269.
- (40) Perticaroli, S.; Comez, L.; Paolantoni, M.; Sassi, P.; Morresi, A.; Fioretto, D. *J. Am. Chem. Soc.* **2011**, *133*, 12063–12068.
- (41) Fioretto, D.; Scarponi, F. *Mater. Sci. Eng., A* **2009**, *521*–22, 243–246.
- (42) Lupi, L.; Comez, L.; Paolantoni, M.; Fioretto, D.; Ladanyi, B. M. *J. Phys. Chem. B* **2012**, *116*, 7499–7508.
- (43) Smith, W.; Forester, T. R. *DL_poly 2*, CCLRC, Daresbury Laboratory, Daresbury, UK.
- (44) Smith, W.; Todorov, I. T. *Mol. Simul.* **2006**, *32*, 935–943.
- (45) Berendsen, H. J. C.; Grigera, J. R.; Straatsma, T. P. *J. Phys. Chem.* **1987**, *91*, 6269–6271.
- (46) Damm, W.; Frontera, A.; TiradoRives, J.; Jorgensen, W. L. *J. Comput. Chem.* **1997**, *18*, 1955–1970.
- (47) Ciccotti, G.; Ferrario, M.; Ryckaert, J. P. *Mol. Phys.* **1982**, *47*, 1253–1264.
- (48) Allen, M. P.; Tildesley, D. J. *Computer Simulation of Liquids*; Oxford University Press: New York, 1987.
- (49) Fioretto, D.; Marini, A.; Massarotti, M.; Onori, G.; Palmieri, L.; Santucci, A.; Socino, G. *J. Chem. Phys.* **1993**, *99*, 8115–8119.
- (50) Torre, R.; Bartolini, P.; Righini, R. *Nature* **2004**, *428*, 296–299.
- (51) Teixeira, J.; Luzar, A.; Longeville, S. J. *Phys.: Condens. Matter* **2006**, *18*, S2353–S2362.
- (52) Laage, D.; Stirmemann, G.; Hynes, J. T. *J. Phys. Chem. B* **2009**, *113*, 2428–2435.
- (53) Lupi, L.; Comez, L.; Masciovecchio, C.; Morresi, A.; Paolantoni, M.; Sassi, P.; Scarponi, F.; Fioretto, D. *J. Chem. Phys.* **2011**, *134*, 055104.
- (54) Comez, L.; Lupi, L.; Morresi, A.; Paolantoni, M.; Sassi, P.; Fioretto, D. *J. Chem. Phys.* **2012**, *137*, 114509.
- (55) Lupi, L.; Comez, L.; Paolantoni, M.; Sassi, P.; Morresi, A.; Fioretto, D. In *Sucrose: Properties, Biosynthesis, and Health Implications*; Magazù, S., Ed., in press.
- (56) Lupi, L. *Nuovo Cimento Soc. Ital. Fis., C* **2012**, *10.1393/ncc/i2012-11313-11317*.
- (57) Sidebottom, D. L.; Tran, T. D. *Phys. Rev. E* **2010**, *82*, 051904.
- (58) Verde, A. V.; Campen, R. K. *J. Phys. Chem. B* **2011**, *115*, 7069–7084.